Experimental Study of the $T = T_z$ States in ^{90}Zr via a (^{3}He, d) Reaction*

GEORGE VOURVOPOULOS

Department of Physics, Florida A&M University, Tallahassee, Florida and Department of Physics, Florida State University, Tallahassee, Florida 32306

AND

J. D. FOX†

Department of Physics, Florida State University, Tallahassee, Florida 32306

(Received 11 July 1968)

^{89}Y(^{3}He, d)^{90}Zr data taken with the Oak Ridge isochronous cyclotron with $E^3_{He}=25$ MeV are analyzed. 35 states are observed between 5.08- and 8.12-MeV excitation with $l_p=2$ and $l_p=0$. These states are considered to be the antianalog single-particle–hole states of the $p_{1/2}^{-1}d_{5/2}$, $p_{1/2}^{-1}s_{1/2}$, and $p_{1/2}^{-1}d_{3/2}$ proton configuration in ^{90}Zr mixed with "core-polarization" states. The possibility exists that there are some additional states of the $p_{1/2}^{-1}d_{3/2}$ proton configuration higher than 8.12 MeV. The energy separation between the centroid of each of the $T_<=T_0-\frac{1}{2}$ groups and the corresponding analogs with $T_>=T_0+\frac{1}{2}$ is found to be approximately 7 MeV. The strength of the isobaric-spin-dependent potential, responsible for the splitting of the $T_<$ from the $T_>$ states, is calculated to be 148 MeV. Spectroscopic factors are extracted and are compared with theoretical sums of spectroscopic factors. The total number of $T_<$ states seen is in good agreement with the number calculated from considerations of core-polarization states mixed with the antianalog states through nuclear interactions.

I. INTRODUCTION

THE addition of a proton to a nucleus can lead to the formation of states (p+target) which are the isobaric analog states of the low-lying states of the (n+target) system, where p and n denote proton and neutron, respectively. These (p+target) analog (or $T_>$) states have the same isobaric spin T as the (n+target) states but differ in the T_Z component, and are considered to be members of the same isobaric-spin multiplet.

However, the addition of a proton leads also to the formation of states that have isobaric spin $T-1$. Some of these states are of particular interest because they have (ideally) the same shell-model configuration with the analog states except for a difference in weighting factors. We call these states antianalog states. From this definition it is implied that for each analog state there is only one antianalog state. However, the antianalog state shares its strength through residual interactions with other complicated nuclear configurations (e.g., "core-polarization" states) that have the same spin and parity. This results in the manifestation of a number of states that we call $T_<$ states. The sharing of the strength of the antianalog state with the $T_<$ states results in a distribution similar to that of a giant resonance. The $T_<$ states have $T_<=T_z$, but it should be pointed out that there can be other nuclear states with $T=T_z$ that do not belong to any of the $T_<$ groups, e.g., all the $l_p=1$ and $l_p=4$ transitions in the present experiment. The $T_<$ states are located several MeV below the corresponding $T_>$ ones and in many cases are formed as bound states. The study of these bound $T_<$ states can therefore be accomplished only through reactions that lead to the configuration (p+target) with the proton captured in an energy level below the proton separation energy. Figure 1 pictorially shows a (p, p) reaction resulting in the formation of the $T_>$ states only and a (^{3}He, d) reaction forming both $T_>$ and $T_<$ states.

$T_<$ states have been observed in a number of one-particle transfer reactions. For some of these experiments, see Ref. 1. These experiments, however, do not discuss in detail the fragmentation of the antianalog states. The present experiment ^{89}Y(^{3}He, d)^{90}Zr was performed with the purpose of forming and subsequently investigating the mechanism of formation of the $T_<$ states. A preliminary report of these findings has already appeared.[2] Section II describes the experimental procedure and Sec. III presents the experimental results and their analysis. Section IV presents a discussion of the results and a comparison with theoretical calculations concerning the number of observed states and their spectroscopic strength. Section V contains a summary of the experimental observations.

II. EXPERIMENTAL PROCEDURE

Data were taken using the 25-MeV ^{3}He beam from the Oak Ridge isochronous cyclotron. Deuterons from

* Supported in part by the U.S. Air Force Office of Scientific Research, Office of Aerospace Research, U.S. Air Force, under AFOSR Grant No. AF-AFOSR-440-67, the National Science Foundation under Grant No. NSF-GP-5114, and the U.S. Atomic Energy Commission under contract with Union Carbide Corporation.

† Present address: Max-Planck-Institut für Kernphysik, Heidelberg, Germany.

[1] R. Sherr, B. F. Bayman, E. Rost, M. E. Rickey, and C. G. Hoot, Phys. Rev. **139**, B1272 (1965); D. D. Armstrong and A. G. Blair, *ibid.* **140**, B1226 (1965); B. Rosner and D. J. Pullen, *ibid.* **162**, 1048 (1967).

[2] G. Vourvopoulos and J. D. Fox, Phys. Letters **25B**, 543 (1967).

the reaction were recorded in nuclear emulsion plates (Kodak NTB 50 μ) placed along the focal plane of the Oak Ridge broad-range spectrograph. This spectrograph is a uniform single-wedge magnet, of the type described by Elbek and his co-workers.[3] To prevent any α particles from registering on the plates, Al foils were placed in front of the plates. Four nuclear emulsion plates were used at each angle, thus obtaining a 16-MeV deuteron energy range. A self-supported ^{89}Y foil, 292 μg/cm^2, was used.[4] The thickness of the foil was determined by weighing and by elastic scattering of low-energy protons from it. Spectra were measured at 12 angles: 5°, 7.5°, and in 5° intervals from 10° to 55°. The spectrograph magnetic field was 8.5 kG, the acceptance angle was 3° in the reaction plane, and the solid angle along the focal plane varied between 9×10^{-4} (low-energy end) and 5×10^{-4} sr (high-energy end). The beam was monitored by a beam-current integrator and a monitor counter placed at 30°, to detect elastically scattered ^{3}He particles.

The over-all energy resolution (full width at half-maximum) in the outgoing deuteron spectrum was found to be about 30 keV.

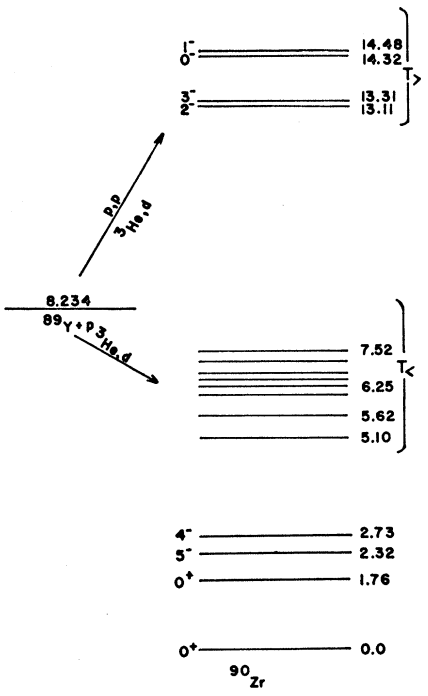

FIG. 1. Graphical representation of the ^{89}Y(p, p) and ^{89}Y(^{3}He, d)^{90}Zr reaction. The elastic scattering can only lead to $T_>$ and $T_<$ states which are unbound, while the (^{3}He, d) reaction allows the investigation of the bound $T_<$ states.

[3] J. Borggreen, B. Elbek, and L. P. Nielson, Nucl. Instr. Methods **24**, 1 (1963).

[4] Supplied by Frank J. Karasek, Microfoils, Inc., Argonne, Ill.

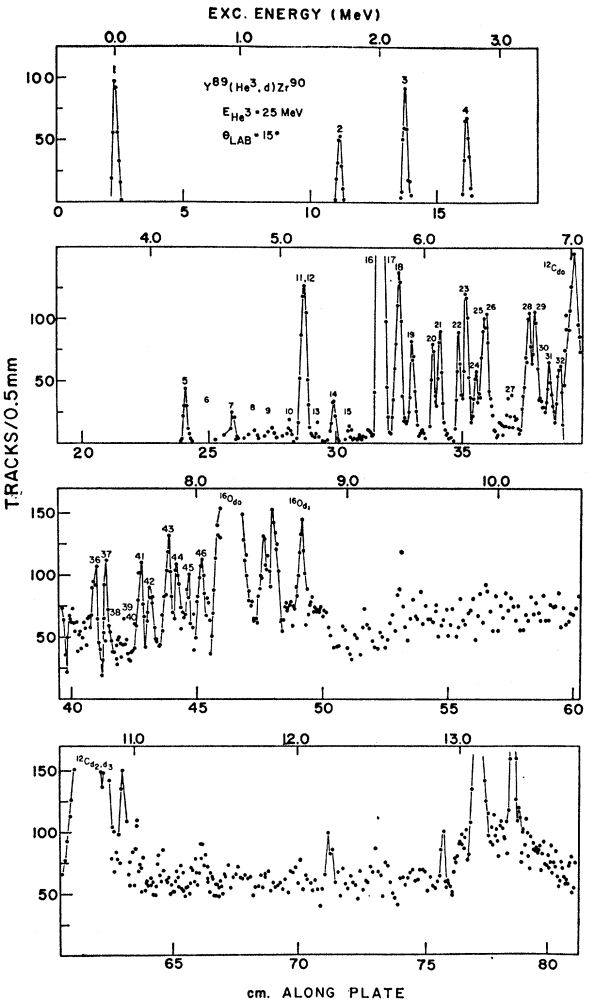

FIG. 2. Deuteron spectrum obtained at 15°. Solid lines are not fits to the data, but are drawn to accentuate the peaks. Impurity peaks are labeled with respect to impurity target nucleus.

III. EXPERIMENTAL RESULTS AND ANALYSIS

A typical spectrum from the present experiment is the deuteron spectrum taken at 15° and shown in Fig. 2. As can be seen, level structure was obtained up to about 14-MeV excitation in ^{90}Zr. Although the target was pure ^{89}Y, C and O were built up on the target, resulting in contaminant peaks. Unfortunately, the ground state of ^{13}N formed by the reaction ^{12}C(^{3}He, d)^{13}N was in the midst of the region that contains much information on the $T_<$ states, and its presence made the analysis very difficult.

As shown in Fig. 2, the deuteron groups occur in well-formed peaks up to approximately 7-MeV excitation in ^{90}Zr. Between 7 and 8 MeV, the background is higher and there was considerable difficulty in recognizing the different deuteron peaks from one angle to the other.

TABLE I. ^{3}He elastic scattering parameters. Geometrical parameters: sets A–E: $a=0.7$ F, R_0' (r_0') $=6.92$ (1.55) F, $a'=0.8$ F, R_c (r_c) $=6.27$ (1.4) F; set F: $a=0.75$ F, R_0' (r_0') $=7.0$ (1.568) F, $a'=0.75$ F, R_c (r_c) $=7.0$ (1.568) F. σ_R is the total reaction cross section.

Parameter set	V (MeV)	R_0 (r_0) (F)	W (MeV)	χ^2	σ_R (mb)
A	45	6.2(1.388)	15.0	57	1422
B	80	5.8(1.299)	15.0	40	1424
C	116	5.55(1.243)	15.0	33	1426
D	157	5.35(1.198)	15.0	27	1428
E	208	5.15(1.153)	15.5	20	1435
F	12	7.0(1.568)	18.0	52	1413

Analysis of the data was attempted up to 8.12-MeV excitation. The experimental errors for $d\sigma/d\Omega$ range from 8% for the high-count peaks to 20% for the low-count peaks.

The bulk of the distorted-wave Born approximation (DWBA) calculations were performed with the computer code TSALLY.[5] In the latter stage of the analysis, DWBA codes written by Tamura[6] were used.

The optical model used for both entrance and exit channels is of the form

$$U(r)=-V/(e^x+1) -i[W-4W'(d/dx')](e^{x'}+1)^{-1}+U_c(r),$$

where $U_c(r)$ is the Coulomb potential in its usual form and

$$x=(r-R_0)/a, \quad x'=(r-R_0')/a', \quad R_0=r_0A^{1/3}.$$

For the entrance channel, ^{3}He elastic scattering data at 24.7 MeV were obtained from Preedom.[7] The data were fitted using the optical-model analysis program OPTIX1.[8] The values for the sets of the parameters giving the best fit to the data are given in Table I. Figure 3 contains the ^{3}He elastic scattering data with an optical-model fit to it.

For the exit channel, because of the nonavailability of deuteron elastic scattering data from ^{90}Zr in the energy range 20–28 MeV, parameters derived by Perey and Perey[9] were used. These parameters were obtained from a systematic analysis of the deuteron optical-model interactions in the range of $E_d=11$–27 MeV which shows that, for fixed geometrical parameters, there is a smooth variation of V and W' with energy.

The two sets of parameters as found from this systematic study and for the case of ^{90}Zr are given in Table II. Different combinations of entrance- and exit-channel parameters were tried in the analysis of the present data, but there were no appreciable differences in the shapes of the angular distributions or in the magnitude of the cross sections. In the analysis presented in this paper, parameter set D for the incident ^{3}He and parameter set B for the deuterons were used, since these most closely approximate the three and two nucleon potentials, respectively.

For the bound-state wave function a Woods-Saxon potential was used, and the well depth was adjusted to give the known separation energy. A spin-orbit potential of the form

$$V_{SOR}(\hbar/m_pc)^2r^{-1}(d/dr)(e^x+1)^{-1}2\mathbf{l}\cdot\mathbf{s}$$

was used. The magnitude of the V_{SOR} was taken to be 8 MeV/F^2. The extraction of spectroscopic factor S was accomplished from the relation

$$(d\sigma/d\Omega)_{expt}=4.42[(2J_b+1)/(2J_a+1)]C^2S\sigma_{DWBA},$$

where the factor 4.42 is a normalization factor for (^{3}He, d) reactions,[10] J_b and J_a are the angular momenta

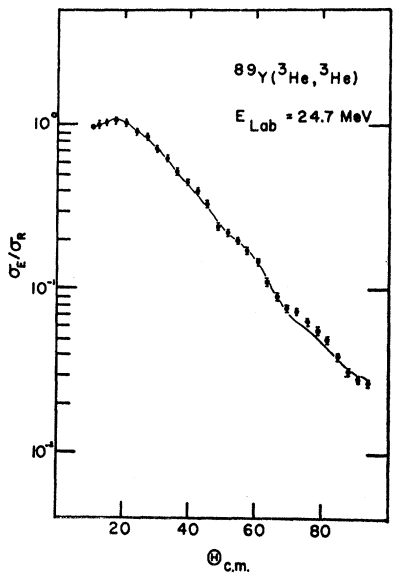

FIG. 3. ^{89}Y(^{3}He, ^{3}He) data (Preedom, Ref. 3) at 24.7 MeV. Solid line represents an optical-model fit to the data.

[5] R. H. Bassel, R. M. Drisko, and G. R. Satchler, Oak Ridge National Laboratory Report No. ORNL-3240, 1962 (unpublished).
[6] T. Tamura (private communication).
[7] B. M. Preedom (private communication).
[8] W. J. Thompson and E. Gille, Florida State University Tandem Accelerator Laboratory Technical Report No. 9, 1965 (unpublished).
[9] C. M. Perey and F. G. Perey, Phys. Rev. **132**, 755 (1963).
[10] R. H. Bassel, Phys. Rev. **149**, 791 (1966).

TABLE II. d elastic scattering parameters. E_d is the deuteron energy; $r_0 = 1.15$ F, $r_c = 1.15$ F.

Parameter set	V (MeV)	W' (MeV)	r_0' (F)	a (F)	a' (F)
A	$71.5-0.51E_d$	$9.1+0.24E_d$	1.37	0.87	0.7
B	$98.8-0.22E_d$	$12.7+0.24E_d$	1.34	0.81	0.68

of the final and initial states, and C is the isobaric-spin Clebsch-Gordan coefficient which accounts for the fact that the captured proton can distribute its strength among states that have the same total angular momentum but different isobaric spin. The last quantity, σ_{DWBA}, is the theoretical prediction of the DWBA cross section as given by the computer code. In the calculations of σ_{DWBA} no lower cutoffs were employed, since it was found that the use of lower cutoffs up to 4 F did not change the stripping cross sections more than 5% in magnitude, and the angular distributions were practically unaltered.

Table III lists the states that resulted from the analysis, the l values of the captured protons, the experimental values of $(2J_b+1)C^2S$, and the theoretical values $\sum(2J_b+1)C^2S$, where the sum extends over all

TABLE III. ^{89}Y(^{3}He, d)^{90}Zr results.

Level No.	E_x (MeV)[a]	l_p	$(2J_b+1)\times C^2S$ Expt.	$\Sigma(2J_b+1)\times C^2S$ Theor.
1	0.0	1	1.31	2.0
2	1.76	1	0.52	
3	2.32	4	12.43	20.0
4	2.73	4	9.99	
5	4.23	1 ($p_{1/2}$)	0.22	
		1 ($p_{3/2}$)	0.18	
6	4.50	1 ($p_{1/2}$)	0.08	
		1 ($p_{3/2}$)	0.06	
7	4.56	1 ($p_{1/2}$)	0.14	
		1 ($p_{3/2}$)	0.11	
8	4.65	1 ($p_{1/2}$)	0.04	
		1 ($p_{3/2}$)	0.04	
9	4.78	1 ($p_{1/2}$)	0.06	
		1 ($p_{3/2}$)	0.04	
10	4.98	2	0.04	
11	5.08	2	0.57	
12	5.10			
13	5.18	1 ($p_{1/2}$)	0.08	
		1 ($p_{3/2}$)	0.06	
14	5.31	2	0.06	
15	5.42	2, 1	0.05, 0.04	
16	5.62	2	1.09	11.0 ($d_{5/2}$)
17	5.66	2	0.38	
18	5.76	2	0.43	
19	5.86	2	0.26	
20	6.02	2	0.16	
21	6.07	2	0.25	
22	6.20	2	0.18	
23	6.25	2	0.33	
24	6.32	2	0.12	
25	6.37	2	0.49	
26	6.40			
27	6.64	2	0.10	
28	6.67	(60%0, 40%2)	0.16 (s)	
29	6.71		0.10 (d)	
30	6.76	2	0.08	
31	6.81	2	0.16	
32	6.88	0	0.12	
33	7.00	0	0.14	
34	7.11	0	0.16	
35	7.16	2	0.17	3.66 ($s_{1/2}$)
36	7.26	0	0.17	
37	7.35	2	0.18	
38	7.42			
39	7.48			
40	7.53	2	0.36	
41	7.58			
42	7.65	2	0.25	7.33 ($d_{3/2}$)
43	7.77	2	0.26	
44	7.84	2	0.26	
45	7.91	2	0.23	
46	8.00			
47	8.05	2	0.19	
48	8.12	2	0.37	

[a]Excitation energy error ±15 keV.

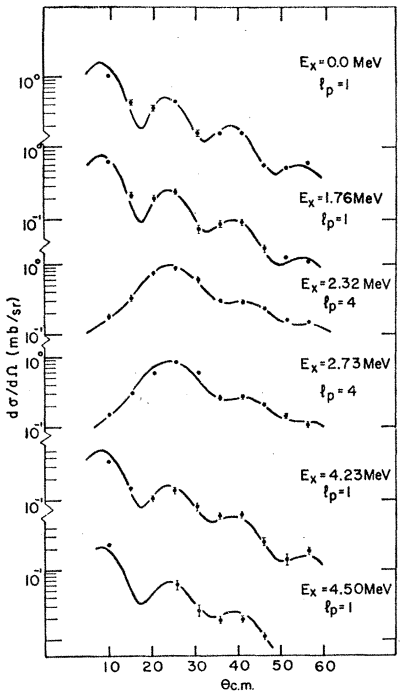
E_x=0.0 MeV
ℓ_p=1
E_x=1.76MeV
ℓ_p=1
E_x=2.32 MeV
ℓ_p=4
E_x=2.73MeV
ℓ_p=4
E_x=4.23MeV
ℓ_p=1
E_x=4.50MeV
ℓ_p=1
dσ/dΩ (mb/sr)
θc.m.

(a)

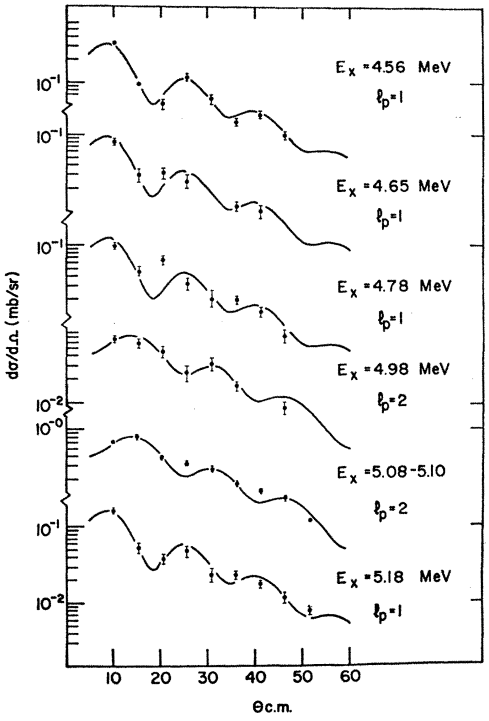
E_x=4.56 MeV
ℓ_p=1
E_x=4.65 MeV
ℓ_p=1
E_x=4.78 MeV
ℓ_p=1
E_x=4.98 MeV
ℓ_p=2
E_x=5.08-5.10
ℓ_p=2
E_x=5.18 MeV
ℓ_p=1
dσ/dΩ (mb/sr)
θc.m.

(b)

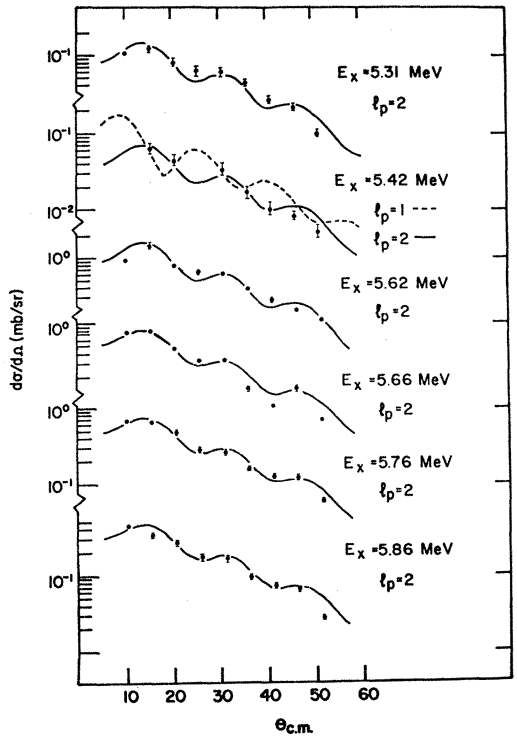
E_x=5.31 MeV
ℓ_p=2
E_x=5.42 MeV
ℓ_p=1 ---
ℓ_p=2 —
E_x=5.62 MeV
ℓ_p=2
E_x=5.66 MeV
ℓ_p=2
E_x=5.76 MeV
ℓ_p=2
E_x=5.86 MeV
ℓ_p=2
dσ/dΩ (mb/sr)
θc.m.

(c)

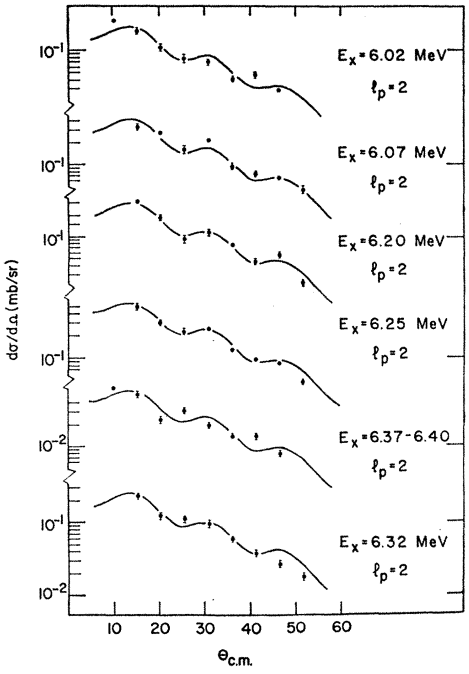
E_x=6.02 MeV
ℓ_p=2
E_x=6.07 MeV
ℓ_p=2
E_x=6.20 MeV
ℓ_p=2
E_x=6.25 MeV
ℓ_p=2
E_x=6.37-6.40
ℓ_p=2
E_x=6.32 MeV
ℓ_p=2
dσ/dΩ (mb/sr)
θc.m.

(d)

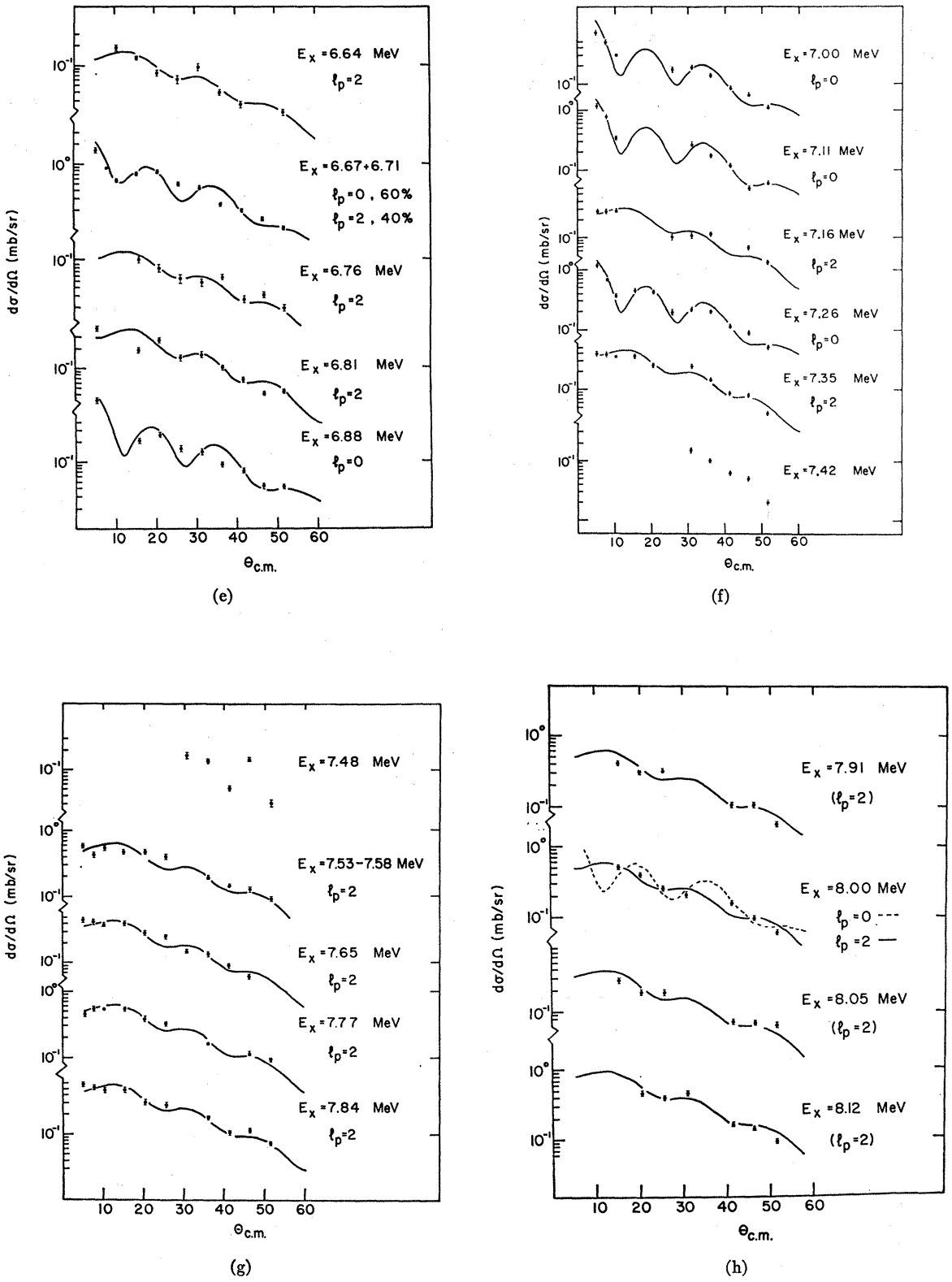

FIG. 4. Deuteron angular distributions. Smooth curves are DWBA predictions. Error bars, where not shown, are the size of the data points.

the states that are formed from the capture of the proton in the same shell. The sum rule for the spectroscopic factors is the one developed by French and Macfarlane.[11] Figures 4(a)–(h) present the angular distributions of the deuteron groups analyzed, together with the DWBA fits to the data.

IV. DISCUSSION

The ground state (g.s.) and the first three low-lying states in ^{90}Zr have previously been investigated,[12,13] and since our results are in good agreement with the previous results, additional discussion is not necessary.

A. $l_p=1$ Transitions

Between 4.23 and 5.18 MeV in ^{90}Zr, six levels were observed with a shape characteristic of an $l_p=1$ captured proton. The strongest of these levels is the one observed at 4.23 MeV. Evidence for the existence of this level is in the (^{3}He, d) data of Day *et al.*[13] but is not referred to in the text. This state has previously been observed in a ^{90}Zr(p, p') experiment and has spin 5^- assigned to it.[14] However, other experiments assign to it a spin of 2^+,[15] and the present results rule out the 5^- assignment. If it is assumed[12,16] that the capture of a proton by an ^{89}Y core with the configuration $[(p_{3/2})_0{}^4p_{1/2}]_{1/2^-}$ exhausts all its strength in the formation of the ground state and the 1.76 state in ^{90}Zr, then the existence of $l_p=1$ states at higher excitation energies in ^{90}Zr would imply that the ground state of ^{89}Y contains admixtures of other configurations. The simplest configuration[15] admixed into the $[(p_{3/2})_0{}^4p_{1/2}]_{1/2^-}$ configuration would be $\{[(p_{3/2})^{-2}(g_{9/2})_0{}^2]_0p_{1/2}\}_{1/2^-}$ and the addition of a $p_{3/2}$ proton yields

$$\{(g_{9/2})_0{}^2[(p_{3/2})^{-1}p_{1/2}]\}_{1^+,2^+}.$$

The addition of a $p_{1/2}$ proton would give

$$\{(g_{9/2})_0{}^2[(p_{3/2})^{-2}(p_{1/2})^2]\}_{0^+}$$

and these states would be formed in higher excitation in ^{90}Zr than the 1^+ and 2^+. Because the angular distributions for the present experiment were taken up to 55° only, differentiation between states of $l_p=1$ but different total angular momentum is not possible. This is indicated in Table III, where the $l_p=1$ states are shown as $(p_{1/2})$ and $(p_{3/2})$. The conclusions that we can therefore draw from the present data are that there is evidence that the ground state of ^{89}Y is not a pure single-particle state, but contains admixtures of other configurations, with the possibility of the most prominent one being the $\{[(p_{3/2})^{-2}(g_{9/2})^2]_0p_{1/2}\}_{1/2^-}$ admixture.

B. $T_<$ States

From 5.08 to 8.12 MeV in ^{90}Zr, a total of 35 states were observed with shapes characteristic of $l_p=2$ and $l_p=0$ for the captured proton. It is our belief that these states are the antianalog states (mixed with other complicated nuclear configurations) of the states in ^{90}Zr at 13.11-, 13.31- ($J^\pi=2^-$, 3^-), 14.32-, 14.48- ($J^\pi=0^-$, 1^-), and 15.61-, 15.74-MeV ($J^\pi=2^-$, 1^-) excitation. The states at 13.11 MeV, etc., in ^{90}Zr are the analog states of the low-lying states in ^{90}Y, formed by capture of a $d_{5/2}$, $s_{1/2}$, or $d_{3/2}$ protons by the ^{89}Y core.

From 5.08- to 7.00-MeV excitation, we see many states with $l_p=2$ that correspond to the $T_>$ states at 13.11 and 13.31 MeV. Around 7.2 MeV we see several $l_p=0$ states, corresponding to the $T_>$ states at 14.32 and 14.48 MeV. Above 7.3 MeV we observe states that have $l_p=2$ shape again and probably correspond to the $T_>$ states at 15.61 and 15.74 MeV. These three groups will be referred to from now on as $d_{5/2}T_<$, $s_{1/2}T_<$, and $d_{3/2}T_<$ groups. To discuss the formation of the $T_<$ states, consider the specific example of ^{89}Y as a target and the addition of a proton resulting in the formation of the state in ^{90}Zr which is the analog state of the ground state of ^{90}Y. The ground state of ^{90}Y will be assumed to be the (^{89}Y+neutron) or $|\,nC\rangle$ system. Assuming that the target, ^{89}Y, has pure isobaric spin $T_0=T_{0z}$ and neglecting antisymmetrization requirements for the extra nucleon, we can write[17]

$$|\,nC\rangle = |\,T_0T_0;\tfrac{1}{2}\tfrac{1}{2}\rangle = |\,T_0\tfrac{1}{2}T_0+\tfrac{1}{2};\,T_0+\tfrac{1}{2}\rangle.$$

The notation $|\,T_0T_{0z};\,tt_z\rangle$ and $|\,T_0\tfrac{1}{2}T;\,T_z\rangle$ is used to represent the uncoupled and vector-coupled states, respectively. The ground state of ^{90}Y can be pictorially written in the n-p formalism as in Fig. 5, where shaded areas indicate filled shells.

The (^{89}Y+p) system, or $|\,pC\rangle$ system, can also be written as

$$|\,pC\rangle = |\,T_0T_0;\tfrac{1}{2},\,-\tfrac{1}{2}\rangle$$
$$= (2T_0+1)^{-1/2}\,|\,T_0\tfrac{1}{2}T_0+\tfrac{1}{2};\,T_0-\tfrac{1}{2}\rangle$$
$$+(2T_0)^{1/2}\,|\,T_0\tfrac{1}{2}T_0-\tfrac{1}{2};\,T_0-\tfrac{1}{2}\rangle,$$

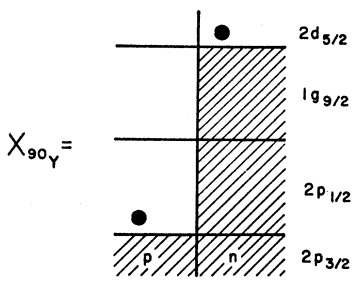

FIG. 5. Pictorial representation, in the n-p formalism, of the ground state of ^{90}Y. Shaded areas indicate filled shells.

[11] J. B. French and M. H. Macfarlane, Nucl. Phys. **26**, 168 (1961).
[12] B. F. Bayman, A. S. Reiner, and R. K. Sheline, Phys. Rev. **115**, 1627 (1959).
[13] R. B. Day, A. G. Blair, and D. D. Armstrong, Phys. Letters **9**, 327 (1964).
[14] W. S. Gray, R. A. Kenefick, J. J. Kraushaar, and G. R. Satchler, Phys. Rev. **142**, 735 (1966).
[15] G. R. Satchler (private communication).
[16] I. Talmi and I. Unna, Nucl. Phys. **19**, 225 (1960).
[17] D. Robson, Phys. Rev. **137**, B535 (1965).

where the statistical factors are Clebsch-Gordan coefficients for the vector coupling.

The states in $|pC\rangle$ with $T_>=T_0+\frac{1}{2}$ are the isobaric analog states of the $|nC\rangle$ system, and the states with $T_<=T_0-\frac{1}{2}$ are the antianalog states. We can expand the analog and antianalog states in the uncoupled representation

$$|T_0\tfrac{1}{2}T_>;\ T_0-\tfrac{1}{2}\rangle=(2T_0+1)^{-1/2}[\,|pC\rangle+(2T_0)^{1/2}\,|nA\rangle]$$

and

$$|T_0\tfrac{1}{2}T_<;\ T_0-\tfrac{1}{2}\rangle=(2T_0+1)^{-1/2}[(2T_0)^{1/2}\,|pC\rangle-|nA\rangle],$$

where $|A\rangle=|T_0T_0-1\rangle$ is the isobaric analog of the target state $|T_0T_0\rangle$.

In a pictorial form the 2^- and 3^- $T_>$ states in ^{90}Zr can be written as in Fig. 6.

The appropriate pictorial representation of the corresponding antianalog states in ^{90}Zr is given in Fig. 7.

As can be seen from these representations, the first part of the $\chi^{>^{90}\mathrm{Zr}}$ differs by an interchange of a neutron with a proton from the ground state of ^{90}Y. Furthermore, apart from the weighting factors involved, $\chi^{>^{90}\mathrm{Zr}}$ and $\chi^{<^{90}\mathrm{Zr}}$ have the same shell-model configurations. In both of them the first part corresponds to the single-particle state $|pC\rangle$ and the second and third parts to the more complicated configuration $|nA\rangle$. Let us specifically examine the second part of the $\chi^{<^{90}\mathrm{Zr}}$ representation, shown in Fig. 7. This $|nA\rangle$ configuration involves an n-p interchange but the n-p particle-hole pair has angular momentum $J_0=0$, because the interchange does not affect the angular momentum.[18]

However, there is another set of states, "core-polarization" states, in which the particle-hole pair no longer couples to $J_0=0$. Since these states must couple also to the $p_{1/2}$ proton and the $d_{5/2}$ neutron, the following total J values result: (12), $(11)^3$, $(10)^5$, $(9)^7$, $(8)^9$, $(7)^{11}$, $(6)^{12}$, $(5)^{12}$, $(4)^{12}$, $(3)^{11}$, $(2)^9$, $(1)^6$, and $(0)^2$ (for $J_0\neq0$), where the superscripts denote the number of states having the same J. Since we are interested in the states resulting in $J^\pi=2^-$ and 3^- (we are not able to distinguish between them), we see that a total of 20 core-polarization states can be formed. If the $J^\pi=2^-$ and 3^- $T_<$ states are formed by the process ^{89}Y+proton, then these core-polarization states do not carry any of the strength but can certainly

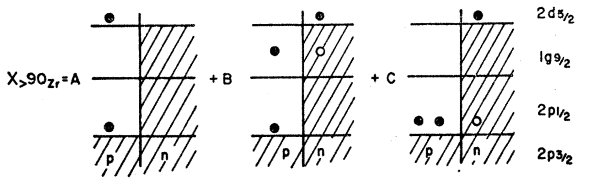

FIG. 6. Pictorial representation, in the n-p formalism, of the 2^- and 3^- $T_>$ states in ^{90}Zr.

[18] J. B. French, in *Proceedings of the International Conference on Nuclear Spectroscopy with Direct Reactions*, edited by F. E. Throw (Argonne National Laboratory, Argonne, Ill., 1964), Report No. ANL-6878, p. 181.

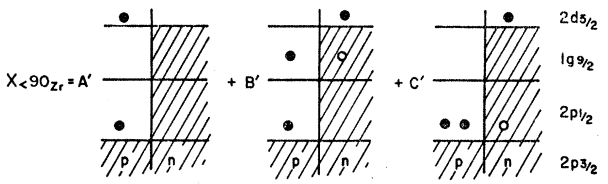

FIG. 7. Pictorial representation, in the n-p formalism, of the corresponding 2^- and 3^- antianalog states in ^{90}Zr.

admix through residual interactions with the $T_<$ states and fragment their strength. Insofar as we consider the second $|nA\rangle$ configuration in the $\chi^{<^{90}\mathrm{Zr}}$ pictorial representation, antisymmetrization allows only $J'=0$ for the two $2p_{1/2}$ protons, and therefore $J=(2)^1$, $(3)^1$. Consequently no core-polarization states arise, and the $J=2$, 3 states are components of the antianalog states. In general, the antianalog state can also mix via the Heisenberg interaction with states involving isobaric spin polarization of the core. In the present case these states are very few and have not been included in the computations.

The quasiparticle configurations $|nA\rangle$ as presented in the description of the $\chi_>$ and $\chi_<$ wave functions represent only what could be called a "first-order complication." A "second-order complication" would involve the interchange of a pair of neutrons and a much larger number of states would be involved with a smaller level spacing. However, calculations of nuclear level density in the region of ^{90}Zr where the $T_<$ states appear[19] show that the states identified here have an energy level spacing comparable to the calculated one, and therefore a higher-resolution experiment probably would not reveal any more structure.

It should be pointed out that these calculations concerning the number of core-polarization states have been simplified with the assumption that the ground state of ^{89}Y is represented by the configuration $[(p_{3/2})_0{}^4p_{1/2}]_{1/2^-}$. The indications, already mentioned, that the ground state contains other admixtures have been neglected.

From angular-momentum considerations we determined that 20 core-polarization states can admix with the antianalog states with $J^\pi=2^-$, 3^- ($l_p=2$). It is not necessary that all these 20 states would admix with the antianalog states. We must find which core-polarization states connect to the antianalog states through nuclear interactions that we assumed to be two-body interactions V_{ij}. We can write the two-body interaction in an irreducible tensor form as

$$V_{12}=\sum_{skr,s'k'} V_{ss'kk',r}(r_1,r_2)[\mathbf{T}^{(sk)r}(1)\cdot\mathbf{T}^{(s'k')r}(2)],$$

where $\mathbf{T}^{(sk)r}$ is an irreducible tensor operator of degree r built out of a tensor of degree s of the spin coordinates and a tensor of degree k of the angular coordinates. Since we are only interested in the angular-momentum part of the interaction, we must examine matrix ele-

[19] T. D. Newton, Can. J. Phys. **34**, 806 (1956).

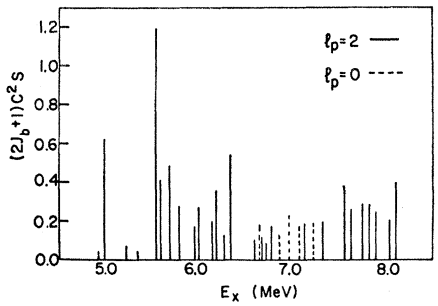

FIG. 8. Experimental $(2J_b+1)C^2S$ versus excitation energy.

ments of the form

$$\langle\psi_{J\neq 0} \mid \mathbf{T}^{(sk)r}(1)\cdot\mathbf{T}^{(s'k')r}(2) \mid \psi_{J=0}\rangle,$$

where V_{12} would be

$$V_{(d_{5/2})(g_{9/2})}, \qquad V_{(g_{9/2})(g_{9/2})}, \qquad V_{(g_{9/2})(p_{1/2})}.$$

Carrying out the evaluation of the matrix elements, it is found that 19 core-polarization states can admix with the antianalog states (for $J^\pi=2^-$, 3^-, $l_p=2$). We see that there is one less state than the number of states found from angular-momentum coupling of the particles and hole in ^{90}Zr.

Carrying out similar calculations for the number of core-polarization states in the case of capture of a $d_{3/2}$ proton and an $s_{1/2}$ proton, we find that there are 11 and 3 core-polarization states, respectively, which can admix with the antianalog states. If we also include the antianalog states, we should have 21 states formed by capture of a $d_{5/2}$ proton ($J^\pi=2^-$, 3^-), 13 states formed by capture of a $d_{3/2}$ proton ($J^\pi=2^-$, 1^-), and 5 states formed from an $s_{1/2}$ proton ($J^\pi=0^-$, 1^-).

In the present experiment, we observe 30 $l_p=2$ states and 5 $l_p=0$ states. Taking into consideration the facts that, in general, the data over 7.00-MeV excitation were very hard to analyze and the presence of the impurity peaks hindered the analysis considerably, it is gratifying that the number of states observed is close to the upper limit of the number of states predicted from the above assumptions.

Figure 8 presents a plot of $(2J_b+1)C^2S$ versus excitation energy, in the energy region over which the spreading of the $T_<$ states occurs. The possibility should also be mentioned of antianalog states in ^{90}Zr whose analogs are formed not as [^{89}Y(g.s.)+proton], but as (^{89}Y*+proton). These last states would be very weakly excited in the present experiment and in a (p, p) experiment,[20] but they manifest themselves in a ^{89}Y(p, p') experiment.[21] The antianalog states formed with an excited ^{89}Y core could admix with core-polarization states also, but the resulting states would have small strength.

C. Spectroscopic Factors

Because of the ambiguity in l_p assignments for a number of states, it is not possible to extract an accurate experimental sum of the $(2J_b+1)C^2S$ for each of the $T_<$ groups. Assuming that the $l_p=2$ states up to 7.16 MeV belong to the $d_{5/2}$ $T_<$ group, the experimental sums of the spectroscopic factors are given in Table IV.

Comparison of the experimental sums to the theoretical sums shows that there is not very good agreement between them. Although the summation was performed under somewhat arbitrary conditions, concerning the differentiation of $d_{5/2}$ and $d_{3/2}$ states, even more accurate experimental summations would only improve the present results very little. In a recent paper[22] the $\mathbf{t}\cdot\mathbf{T}_0$ interaction was employed, providing correction terms to the DWBA amplitude for (^{3}He, d) reactions leading to $T_<$ and $T_>$ states. Because of this interaction, the bound-state wave function ψ_p describing the relative motion of the captured proton with respect to ^{89}Y should be obtained from Lane's coupled-channel equations[23]

$$(T_k-E_p+V_c+V_0-\tfrac{1}{2}T_0V_1/A)\psi_p=-(\tfrac{1}{2}T_0)^{1/2}(V_1/A)\psi_n,$$

$$[T_k-E_p+\Delta_c+V_0+\tfrac{1}{2}(T_0-1)V_1/A]\psi_n = -(\tfrac{1}{2}T_0)^{1/2}(V_1/A)\psi_p.$$

Calculations for ψ_p as given from the coupled-channel equations were performed using Tamura's computer code NEPTUNE, with $V_0=57$ MeV and $V_1=130$ MeV and for excitation energy 5.3 MeV in ^{90}Zr.

Figure 9 shows the bound-state wave function as calculated with the separation-energy method and with the coupled-channel calculations. Subsequent distorted-wave calculations for both cases revealed no more than a 6% difference between the cross sections calculated from the two methods.

TABLE IV. Spectroscopic results.

Group	$\Sigma(2J_b+1)C^2S$ Expt.	Theor.	$E<$ (MeV)	$E>-E<$ (MeV)
$d_{5/2}$	5.05	11.0	6.0	7.2
$s_{1/2}$	0.76	3.66	7.2	7.2
$d_{3/2}$	2.10	7.33	8.0	7.6

[20] C. F. Moore, Ph.D. thesis, Florida State University, 1964 (unpublished).
[21] D. D. Long and J. D. Fox, Phys. Rev. **167**, 1131 (1968).
[22] Taro Tamura, Phys. Rev. **165**, 1123 (1968).
[23] A. M. Lane, Nucl. Phys. **35**, 676 (1962).

D. $T_>$-$T_<$ Energy Separation

The centroid of each group of the $T_<$ states is calculated through the expression

$$E=[\sum E_i S_i(2J_b+1)_i C^2/\sum S_i(2J_b+1)_i C^2],$$

where E_i and S_i refer to the excitation energy and spectroscopic factor of the states comprising each group.

Table IV contains the calculated centroid location of each $T_<$ group and the energy separation between $T_>$ and $T_<$ states. We can see from the table that the energy separation for the $d_{3/2}$ $T_<$ group is a little larger than the others, but the possibility exists of $d_{3/2}$ states of higher excitation energy than 8.12 MeV, where the present analysis was terminated. The proton separation energy is 8.23 MeV and, as can be seen in Fig. 2, there is a considerable background in that region in addition to deuteron groups from ^{16}O(^{3}He, d)^{17}F.

Knowledge of the position of the analog state and the centroid of the $T_<$ states enables us to calculate the value of the potential V_1 appearing in Lane's coupled equations and which is responsible for the splitting of the $T_>$ from the $T_<$ states. If $V_>=V_0+\frac{1}{2}T_0V_1/A$ is the potential for the $T_>$ states and $V_<=V_0-\frac{1}{2}(T_0+1)V_1/A$ is the potential for the $T_<$ states, then $V_>-V_<=(T_0+\frac{1}{2})V_1/A$. To determine $V_>$ for the 13.11-MeV state in ^{90}Zr, which is the analog of the ground state of ^{90}Y, we used a Woods-Saxon potential and adjusted the depth of the potential to give the ground state of ^{90}Y. For the case of $V_<$ the potential was adjusted to give the $d_{5/2}$ state in ^{90}Zr at the centroid position of 6.0-MeV excitation. We found $V_>=-49.9$ MeV and $V_<=-59.9$ MeV, which results in $V_1=148$ MeV. Calculations were carried out in a similar way for the $d_{3/2}$ and $s_{1/2}$ $T_<$ and $T_>$ states, and the value of V_1 was not different by more than 10% from the value of V_1 mentioned above.

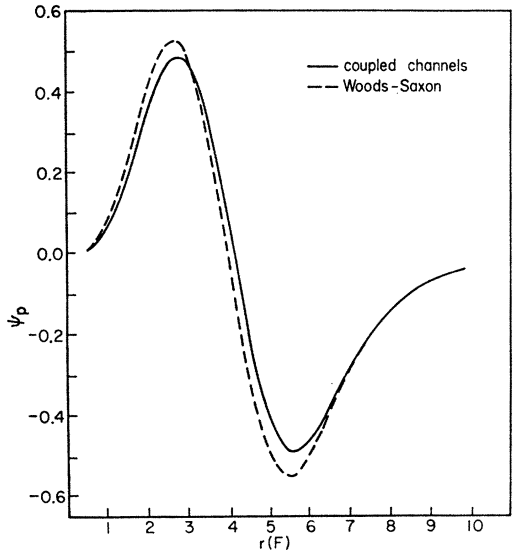

FIG. 9. Radial form factor ψ_p for a proton bound to ^{89}Y with $l_p=2$, forming a 5.3-MeV level in ^{90}Zr.

This value would, of course, change with a more accurate summation of the $d_{5/2}$ states, but this change should not appreciably lower the value of V_1, which is considerably higher than 109 MeV, determined from charge-exchange experiments.[24]

V. SUMMARY

It has been shown that each of the antianalog states formed through the reaction ^{89}Y(^{3}He, d)^{90}Zr mixes with core-polarization states. These last states by themselves could not be observed through the (^{3}He, d) reaction. In the case of ^{90}Zr in the n-p representation the core-polarization states are two-particle–one-hole states (if we consider the ^{89}Y nucleus as a core). We therefore observe the mixing of the antianalog state (which is essentially a single-proton state) with its simplest doorway states—the two-particle–one-hole states. The strength distribution has the characteristic behavior of a giant resonance[25] and the widths of the distributions in the present experiment are of the order of 1 MeV. We observe the mixing of three antianalog states, formed through the capture of a $d_{5/2}$, $s_{1/2}$, and $d_{3/2}$ proton, respectively, with core-polarization states, which results in three overlapping groups of states. The experimental sums of the spectroscopic factors for the $T_<$ states are not in good agreement with the theoretical sums, while the agreement was very good for the low-lying states in ^{90}Zr. The energy separation $E_>$-$E_<$ was found to be around 7 MeV and the strength of the potential responsible for the splitting of the $T_>$ states from the $T_<$ states was found to be 148 MeV.

ACKNOWLEDGMENTS

We are indebted to Dr. J. B. Ball and the cyclotron group for their help on the use of the ORIC facilities. We wish to thank Dr. Donald Robson, Dr. Richard Stephen, and Robert Chatwin for many stimulating discussions. The help of William Courtney, Mrs. Geri Sample, and Wayne Holt in carrying out the calculations is greatly appreciated. We wish to thank the Green Magnet scanning group at Florida State University for their careful work.

[24] G. R. Satchler, R. M. Drisko, and R. H. Bassel, Phys. Rev. **136**, B637 (1964).

[25] A. M. Lane, R. G. Thomas, and E. P. Wigner, Phys. Rev. **98**, 693 (1955).